Asymmetrical firing angle modulation for 12-pulse thyristor rectifiers supplying high-power electrolyzers

Álvaro Iribarren, Ernesto L. Barrios, David Elizondo, Pablo Sanchis and Alfredo Ursúa
Institute of Smart Cities (ISC)
Dept. of Electrical, Electronic and Communications Engineering
Public University of Navarre
Campus de Arrosadia
31006 Pamplona, Spain
alvaro.iribarren@unavarra.es

***Abstract*—This paper presents an asymmetrical firing angle modulation strategy for 12-pulse thyristor rectifiers aimed at supplying high-power electrolyzers, which allows to reduce the size of the passive filter and the static compensator (STATCOM) required to comply with grid harmonic regulations and achieve unity power factor. Usually, 12-pulse thyristor rectifiers follow a symmetric modulation strategy in which the same firing angle is applied to both 6-pulse bridges. In this case, large passive ac-side inductances are required to reduce grid current harmonics, which increase the reactive power consumption and thus the required STATCOM size. However, this paper demonstrates that by applying different firing angles to the two 6-pulse bridges it is possible to comply with the harmonic regulation limits using smaller filtering inductances and therefore reducing the STATCOM size. The methodology to find the optimal firing angle values that should be applied in order to minimize the filtering inductance and the STATCOM size for a given electrolyzer is explained. This strategy is validated by simulation, and results show that the required filtering inductance and the apparent power of the STATCOM can be effectively reduced by 62% and 31%, respectively, using this asymmetrical firing angle modulation.**

Keywords—high-power electrolyzers, 12-pulse thyristor rectifier, asymmetrical firing angles

I. INTRODUCTION

In recent years, interest in green hydrogen has grown substantially, driven mainly by the great development of renewable energy systems [1]. There is a variety of methods to produce green (or renewable) hydrogen [2], among which water electrolysis supplied by renewable electricity stands as the main solution [1], [2]. Nowadays, the most mature and established technologies for high-power applications are proton exchange membrane (PEM) electrolysis and alkaline electrolysis (AEL) [3].

Grid-connected water electrolyzers need to be supplied with dc voltages and currents [4], [5], thus requiring ac-dc converters. Currently, most of high-power electrolyzers are supplied by thyristor rectifiers [6], [7]. Their step-down conversion nature and high current capability fits very well with the large dc current demands (thousands of Amperes) and relatively low dc voltages (hundreds of Volts) of industrial-scale electrolyzers [5]. In addition, high efficiency, reliability and reduced costs are other important advantages of these rectifiers [8].

This work is part of the projects PID2019-110956RB-I00 and TED2021-132604B-I00, funded by MCIN/AEI/10.13039/501100011033 and by the European Union NextGenerationEU/PRTR. It has also been supported by Ingeteam Power Technology.

The main disadvantage of thyristor rectifiers is their low power quality caused by the consumption of reactive power and the grid current harmonics [5], [6], [8]. The large deployment of installed electrolyzer capacity that is expected in the upcoming years [9] can imply an increased share of thyristor rectifiers that can affect the power quality of modern power grids if no corrective actions are taken. In order to limit the harmonic distortion and comply with grid harmonic regulations, the use of passive and/or active power filters is required. Furthermore, the consumption of reactive power is usually compensated using a voltage-source converter (VSC) as a static compensator (STATCOM) in order to control the power factor (PF) [10], [11]. The main drawback is that the use of power filters and STATCOM to improve the power quality of thyristor rectifiers considerably increases the overall cost of the system [5], [6].

One of the most common thyristor topologies used for rectifier applications with large current demands, such as water electrolysis, is the 12-pulse parallel thyristor rectifier [8]. An example of this configuration including the required ac-side filtering inductances and the STATCOM is shown in Fig.1. It consists of two 6-pulse bridges connected in parallel to the same dc output, which is particularly suitable for electrolyzers with high current demands. Due to the star and delta connection of the transformer secondaries, only 12n±1 order harmonics are present in the primary-side grid currents. A dc inductance (L_{dc}) is usually included in series with the electrolyzer, but this does not help to mitigate ac-side current harmonics. Furthermore, the size and cost of this L_{dc} can very high due to the large dc current demands. Instead, a direct connection to the electrolyzer with no L_{dc} is possible [12], thus reducing the overall cost of the system. Normally, ac-side inductances (L_{ac}) are used to filter grid currents, but the inductance values required to meet regulation limits such as those defined in IEEE 519-2014 [13] can be very high. These large L_{ac} inductances lead to an increase in the already high consumption of reactive power, which is a major issue for thyristor rectifiers.

In order to compensate the reactive power and achieve unity PF at the point of common coupling (PCC), a STATCOM is usually employed. If a VSC is used for this purpose, it can simultaneously correct the PF and act as an active filter mitigating grid current harmonics [10], [11]. Doing so it is possible to use smaller filtering L_{ac} inductances, thus reducing the consumption of reactive power and therefore the size of this STATCOM. The main limitation is that high-power industrial two-level VSCs usually have relatively low switching frequencies (around 3 kHz) in order to minimize switching losses, therefore the bandwidth of

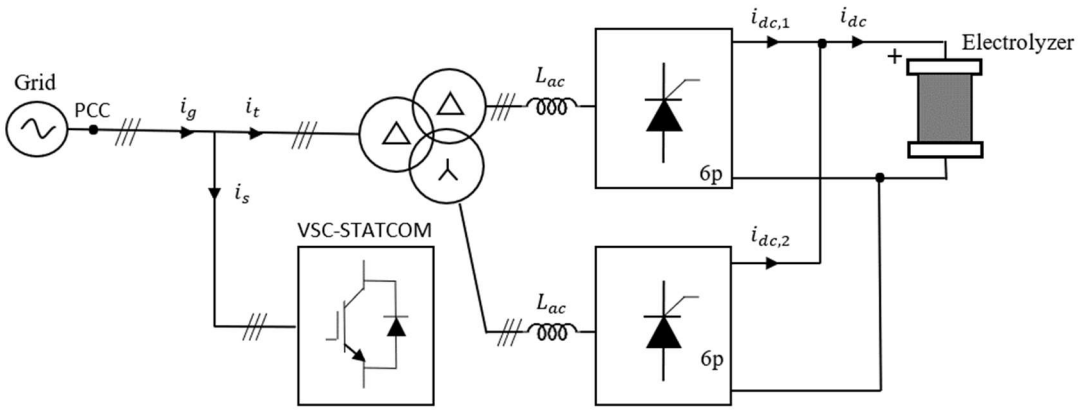

Fig. 1. System circuit diagram showing 12-pulse thyristor rectifier, electrolyzer, L_{ac} inductances and STATCOM.

harmonic frequencies that they can filter is reduced and usually limited to harmonics 5th and 7th [14].

When the same firing angle (α) is applied to the two 6-pulse bridges, harmonics 5th and 7th are not present in the primary-side grid currents. This is called symmetrical firing angle modulation (SFAM), and it is the common practice in most 12-pulse rectifiers as it allows minimizing the total harmonic distortion (THD) of grid currents. However, if an asymmetrical firing angle modulation (AFAM) is followed and different α are applied to the 6-pulse bridges, harmonics 5th and 7th appear and the THD worsens [15], [16], but on the other hand, harmonics 11th and 13th can be reduced. Thanks to this, it is possible to use smaller L_{ac} inductances to filter these 11th and 13th harmonics and comply with their respective regulation limits, while using the VSC-STATCOM to filter the 5th and 7th harmonics. As a consequence, by reducing the L_{ac} inductance with AFAM the reactive power consumed by the thyristor rectifier can be significantly reduced, and therefore also the required STATCOM apparent power.

This paper proposes a methodology that allows finding the optimal AFAM that minimizes the size of the STATCOM required to achieve unity PF, while complying with the grid current harmonic limits established in IEEE 519-2014 regulation, for a 12-pulse rectifier supplying a 5.5 MW electrolyzer. The paper is organized as follows. Section II describes the case study used to validate the proposed AFAM by simulation, including the grid and transformer parameters and the electrolyzer characteristics, and explains how the required STATCOM apparent power can be determined. Section III shows the results of the classical SFAM that is usually employed in 12-pulse rectifiers. In Section IV, the AFAM is described and analyzed. Section V presents the procedure that allows to find the optimal AFAM in order to minimize the passive filtering inductances and the required STATCOM apparent power. Finally, in Section VI, the main conclusions are summed up.

II. System Description

The system configuration of the 12-pulse thyristor rectifier connected to the electrolyzer is depicted in Fig. 1. For this case study, a 5.5 MW PEM electrolyzer is considered. Its electrical behaviour is reproduced using an equivalent electrical model analogous to the one presented in [1], but adjusted with real data from this 5.5 MW electrolyzer. The same electrolyzer was used in [5] by the authors of this work for modelling and analyzing the operation of 6-pulse thyristor rectifiers supplying high-power electrolyzers. The polarization *I-V* curve for this electrolyzer is shown in Fig. 2. The nominal voltage and current of the stack are 790 V and 7000 A, respectively. It also presents a minimum operating current of 700 A below which the electrolyzer is not allowed to operate. This is a safety limit usually established in AEL and PEM electrolyzers in order to prevent the formation of potentially dangerous explosive mixtures of hydrogen and oxygen [1].

In industrial applications, high-power electrolyzers are usually connected to a medium-voltage ac-grid. In this case, a 20 kV grid with a short-circuit ratio (SCR) of 20 is considered. With this SCR, grid current harmonic limits specified in regulation IEEE 519-2014 are the most restrictive (i.e., lowest allowed harmonic amplitude). In this way, it is possible to size the passive current filters and the STATCOM for the most critical scenario.

A transformer with a Ddy configuration is employed. Its delta-star connection of the secondary windings allows for the 12-pulse operation. The primary and secondary nominal phase-to-phase voltages ($U_{T,p}$ and $U_{T,s}$) are adjusted in order to obtain the rated dc voltage and current of the electrolyzer with a firing angle of 0º, as this minimizes reactive power consumption at the nominal operating point [5]. An inductance value of 4 % (in per unit basis) is used for every winding. Furthermore, an X/R ratio of 10 is employed for both the transformer and the grid, as inductive phenomena strongly dominate over resistive losses in high-power applications.

Ac-side inductances L_{ac} are employed to filter grid currents. Their value is determined as the minimal one that allows to comply with the limits established in IEEE 519-2014, not only for the total demand distortion (TDD) but also for every specific harmonic.

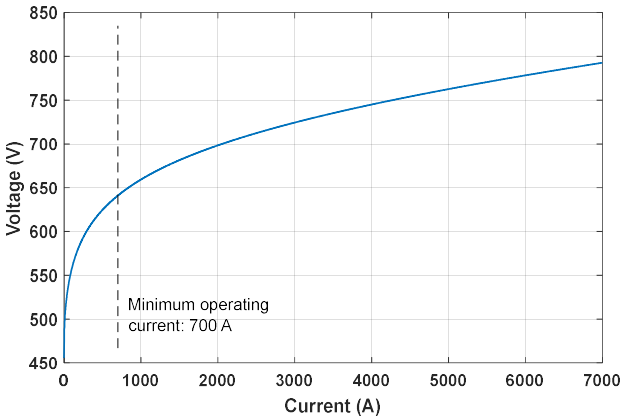

Fig. 2. Polarization $I - V$ curve of the 5.5 MW electrolyzer.

TABLE I. PARAMETERS USED FOR THE VALIDATION BY SIMULATION

CASE	L_{grid} (mH)	R_{grid} $(mOhm)$	$U_{T,p}$ (kV)	$U_{T,s}$ (V)	$L_{T,pD}$ (mH)	$R_{T,pD}$ $(mOhm)$	$L_{T,sy}$ (μH)	$R_{T,sy}$ $(mOhm)$	$L_{T,sd}$ (μH)	$R_{T,sd}$ $(mOhm)$	L_{ac} (μH)
SFAM	10.5	329	20	762	25.1	789	24.3	0.764	72.9	2.29	130
AFAM	10.5	329	20	683	25.1	789	19.5	0.613	58.5	1.84	50

Finally, the STATCOM has to compensate the maximum reactive power that is consumed by the thyristors among the whole operating range of the electrolyzer in order to achieve unity PF. If a SFAM is employed, ac-side current harmonics 5th and 7th of the two thyristor bridges cancel out, but harmonics 11th and 13th appear and cannot be filtered with the STATCOM due to the low switching frequency of industrial-scale VSCs [14]. Therefore, in the case of SFAM, the role of the STATCOM is just to correct the power factor, thus its rated apparent power must be equal to the maximum reactive power consumption of the thyristor rectifier.

On the other hand, if AFAM is used, the STATCOM has to simultaneously compensate reactive power and filter the 5th and 7th current harmonics that arise due to the firing angle imbalance. Contrary to 11th and 13th harmonics, 5th and 7th can be actively filtered by the STATCOM due to their lower frequency. In addition, with an AFAM strategy, 11th and 13th harmonics decrease, and the required L_{ac} inductances to comply with regulation limits can be minimized, and thus the consumption of reactive power. As a consequence, the required apparent power of the STATCOM can be reduced thanks to the AFAM. The set of equations that are used to determine this required STATCOM apparent power (S_s) as a function of both the reactive power consumption of the thyristor rectifier and the amplitude of the 5th and 7th current harmonics can be found in Appendix.

The values of the main parameters that are employed for the validation of the two analyzed study cases (SFAM and AFAM) are recorded in Table I, including grid inductance and resistance (L_{grid} and R_{grid}), transformer phase-to-phase nominal voltages ($U_{T,p}$ and $U_{T,s}$), inductance and resistance of the transformer primary winding ($L_{T,pD}$ and $R_{T,pD}$), star-connected secondary winding ($L_{T,sy}$ and $R_{T,sy}$) and delta-connected secondary winding ($L_{T,sd}$ and $R_{T,sd}$), and filtering inductance L_{ac}.

III. SYMMETRICAL FIRING ANGLE MODULATION (SFAM)

In SFAM the same firing angle α is applied to both 6-pulse thyristor bridges. In this way, the total rectified current (I_{dc}) splits equally between the two 6-pulse bridges:

$$I_{dc,1} = I_{dc,2} = I_{dc}/2. \quad (1)$$

Therefore, they must only be sized for half of the rated electrolyzer power. Fig. 3 shows the relationship between I_{dc} and α with this SFAM. This relationship depends on the electrolyzer polarization curve and the ac-side impedance, as explained in great detail in [5].

When SFAM is employed, only 12n±1 order harmonics are present in the primary-side grid currents due to the star-delta configuration of the transformer secondaries, and the total THD is minimized. The filtering inductance L_{ac} must be sized so that the grid current TDD and all the individual harmonics are within the limits established in IEEE 519-2014. In this case, an inductance of 130 µH is required. This is the value for the 11th harmonic of the grid current ($I_{g,h11}$) to comply with its respective regulation limit, which is a more restrictive condition than the TDD. This is illustrated in Fig. 4, which shows the grid current TDD and the 11th harmonic in percent of I_L (fundamental component of the grid current at the maximum demand load) with this L_{ac} as a function of the firing angle, and compares them to their respective limits defined in IEEE 519-2014.

With this SFAM, as there are no 5th and 7th grid current harmonics, the STATCOM is only used to compensate the reactive power consumed by the thyristor rectifier. Fig. 5 shows the reactive power consumption (Q_t) and the PF at the PCC as a function of the firing angle if no STATCOM was employed. The maximum reactive power is found to be 3.9 MVAr, therefore this must be the rated apparent power of the STATCOM in order to achieve unity PF. Notice that the PF of the thyristor rectifier decreases with increasing α values, but the maximum reactive power consumption happens when α is equal to 0º, that is, at the nominal operating point of the electrolyzer. The reason for this is the large L_{ac} required to filter ac-side currents and comply with regulation limits, which causes a very high reactive power consumption when the electrolyzer is operating at its maximum power (i.e., at its nominal operating point).

IV. ASYMMETRICAL FIRING ANGLE MODULATION (AFAM)

In AFAM different firing angles α_1 and α_2 are applied to the two 6-pulse bridges. There are multiple possible combinations of α_1 and α_2 that yield the same I_{dc} value, as can be seen in Fig. 6a, which shows the contour isolines of I_{dc} as a function of α_1 and α_2. For this case, a L_{ac} inductance of 50 µH has been employed, and the transformer secondary voltage has been determined in order to obtain the nominal electrolyzer current (7000 A) with $\alpha_1 = \alpha_2 = 0$º. As it can be seen, the I_{dc} isolines are symmetrical with respect to the $\alpha_1 = \alpha_2$ line, which corresponds to SFAM. This makes sense, as α_1 and α_2 are interchangeable as long as the ac-side impedances of the two 6-pulse bridges are balanced.

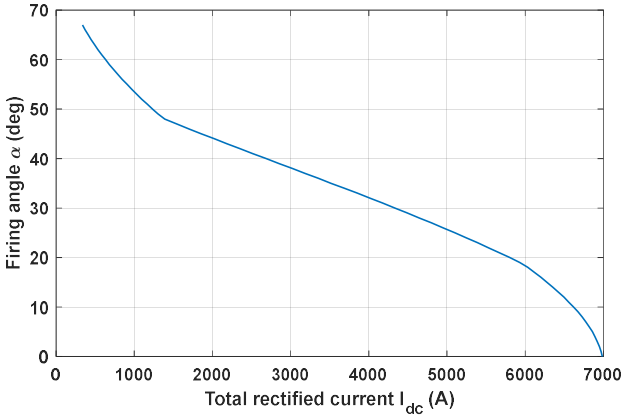

Fig. 3. Required firing angle as a function of the electrolyzer current, using SFAM.

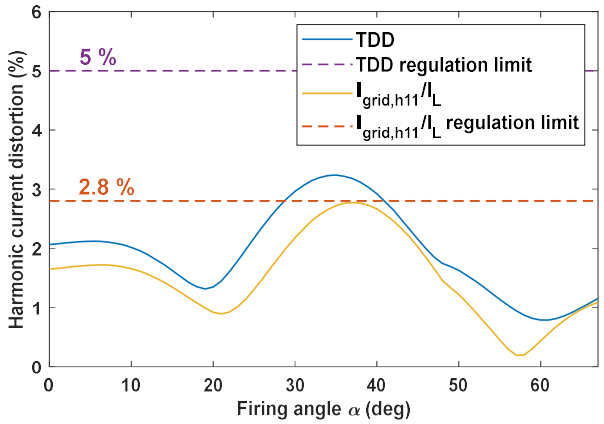

Fig. 4. Grid current TDD and 11th harmonic in percent of I_L as a function of α using SFAM with L_{ac} inductance of 130 µH.

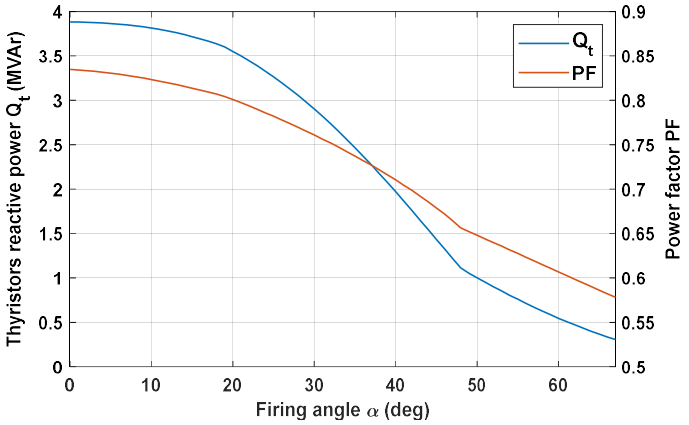

Fig. 5. Reactive power consumption and power factor of the thyristor rectifier as a function of α using SFAM with L_{ac} inductance of 130 µH.

With AFAM, the total rectified current I_{dc} is not shared equally between $I_{dc,1}$ and $I_{dc,2}$. The bridge with a smaller firing angle is the one that presents a higher rectified current. This can lead to α_1 - α_2 combinations where the rectified current of one of the bridges is greater than half of the nominal current of the electrolyzer ($I_{E,nom}$). This is not desired, as this bridge would have to be sized for more than half of the electrolyzer rated power. Fig. 6b shows the contour isolines of $I_{dc,1}$ as a function of α_1 and α_2. The same plot for $I_{dc,2}$ would be obtained by swapping α_1 and α_2.

Fig. 6c presents the 11th harmonic component of the grid current in percent of I_L as a function of α_1 and α_2, corresponding to a L_{ac} inductance of 50 µH. A similar contour plot would be obtained for the 13th harmonic, but with smaller amplitude values due to the greater attenuation of this higher frequency harmonic by the ac-side inductances. As it can be seen, the $\alpha_1 = \alpha_2$ line crosses the 2.8% isoline, which is the limit defined in IEEE 519-2014 for this 11th harmonic. This means that with SFAM and this L_{ac} inductance it is not possible to comply with the regulation limits. However, with AFAM there are many possible $\alpha_1 - \alpha_2$ paths that allow to cover the whole operating range of the electrolyzer while constraining the 11th harmonic below its regulation limit. As the $\alpha_1 - \alpha_2$ combination moves away from the symmetry $\alpha_1 = \alpha_2$ line, the unbalance between $I_{dc,1}$ and $I_{dc,2}$ increases. This causes a reduction of the 11th and 13th harmonics, at the expense of an increase in the 5th and 7th harmonics. This can

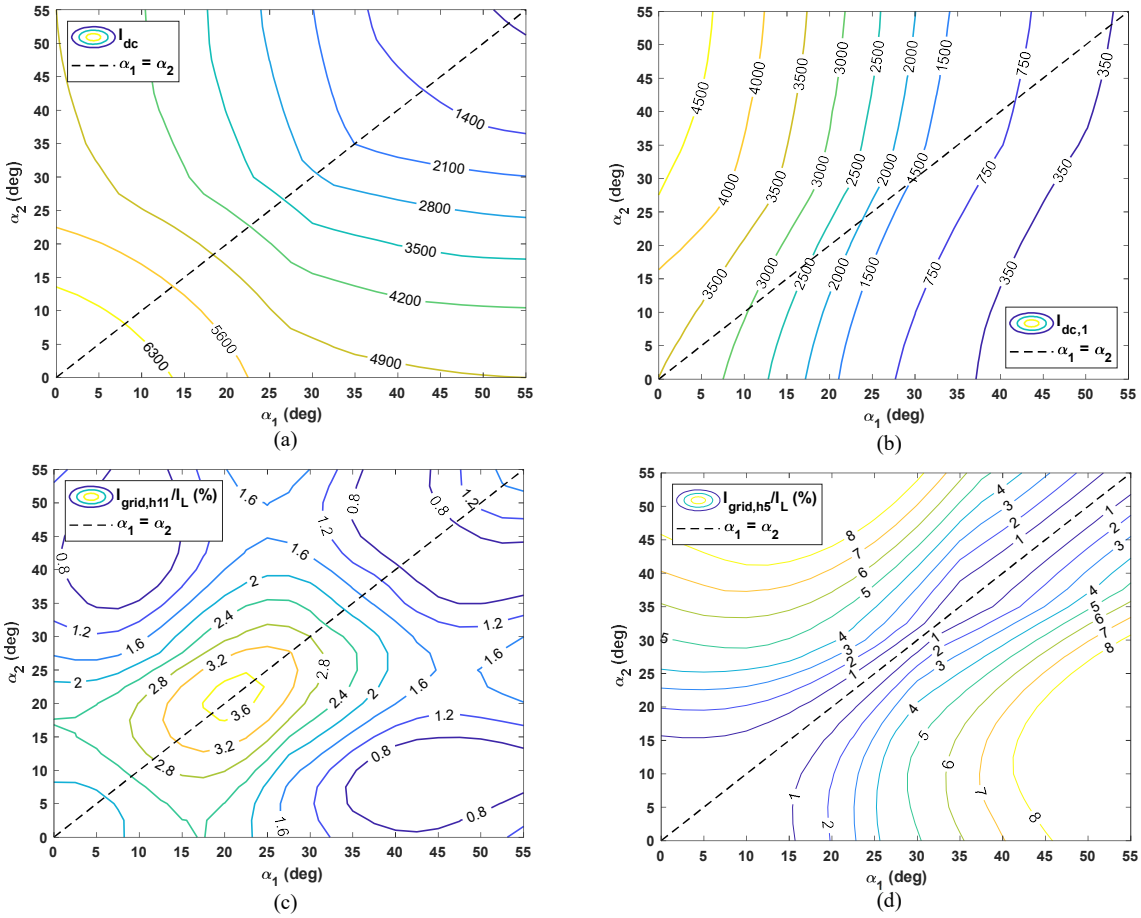

Fig. 6. Contour plots of (a) total rectified current, (b) rectified current of bridge 1, (c) 11th harmonic component of the grid current in percent of I_L and (d) 5th harmonic component of the grid current in percent of I_L, as a function of α_1 and α_2. L_{ac} inductance of 50 µH.

be appreciated in Fig. 6d, which shows the 5th harmonic component of the grid current in percent of I_L as a function of α_1 and α_2. Again, a similar contour plot would be obtained for the 7th harmonic, but with smaller amplitude values due to its higher frequency. These harmonics are not present when SFAM is employed (i.e., through the $\alpha_1 = \alpha_2$ line). They appear when different firing angles are applied to the two 6-pulse bridges, and they increase as the unbalance between $I_{dc,1}$ and $I_{dc,2}$ augments.

V. Optimizaton of Filtering Inductances and Statcom Size Using AFAM

As the 5th and 7th current harmonics can be filtered with the VSC-STATCOM due to their low frequency order, AFAM can be used to reduce the 11th and 13th harmonics and therefore use a smaller L_{ac} to comply with the regulation limits. In order to determine the optimal AFAM $\alpha_1 - \alpha_2$ path to cover the whole operating range of the electrolyzer the following criteria is defined:

- The nominal current of the electrolyzer (i.e., the maximum I_{dc}) must be achieved with $\alpha_1 = \alpha_2 = 0º$, in order to minimize the reactive power consumption at the nominal operating point. To do so, the transformer secondary voltage must be appropriately defined according to the ac-side impedance and the electrolyzer polarization curve, as explained in [5].
- $I_{dc,1}$ and $I_{dc,2}$ must not be greater than $I_{E,nom}/2$ at any operating point. In this way, both 6-pulse bridges can be sized to half of the electrolyzer rated power.
- The 11th grid current harmonic must not surpass the 2.8% regulation limit defined in IEEE 519-2014.
- The $\alpha_1 - \alpha_2$ path must try to minimize 5th and 7th grid current harmonics. Doing so, the required STATCOM power to filter these harmonics will be minimal.
- Finally, in order to ease the controllability of the system, the evolution of I_{dc} along the $\alpha_1 - \alpha_2$ path is set to be monotonic, with only one $\alpha_1 - \alpha_2$ combination for each I_{dc} value.

Following these criteria, the optimal AFAM $\alpha_1 - \alpha_2$ path corresponding to a given L_{ac} can be found. By repeating this process with different L_{ac} values, it is possible to find the minimum inductance that allows to comply with the regulation limit, and therefore minimize the reactive power consumption of the thyristors and the required apparent power of the STATCOM. In this case study, this minimum inductance was found to be 50 µH, which is the one that has been used to obtain the contour plots of Fig. 6.

The optimal AFAM $\alpha_1 - \alpha_2$ path corresponding to this L_{ac} value is shown in Fig. 7. The grey-shaded region represents the $\alpha_1 - \alpha_2$ combinations where either $I_{dc,1}$ or $I_{dc,2}$ are greater than $I_{E,nom}/2$, and the red-shaded area is where the 11th grid current harmonic surpasses the 2.8% regulation limit. The plot also shows the contour isolines of I_{dc}. As it can be seen, the optimal $\alpha_1 - \alpha_2$ path follows the SFAM line ($\alpha_1 = \alpha_2$) whenever the 11th harmonic is below the regulation limit, that is, from $\alpha_1 = \alpha_2 = 0º$ to $\alpha_1 = \alpha_2 = 11º$ (which corresponds to the interval 7000 A > I_{dc} > 5950 A), and from $\alpha_1 = \alpha_2 = 30º$ to $\alpha_1 = \alpha_2 = 55º$ (which corresponds to the interval 2900 A > I_{dc} > 700 A). In these intervals there is no unbalance between $I_{dc,1}$ and $I_{dc,2}$, and therefore no 5th and 7th current harmonics. In the remaining load range, i.e., in the interval 5950 A > I_{dc} > 2900 A, the

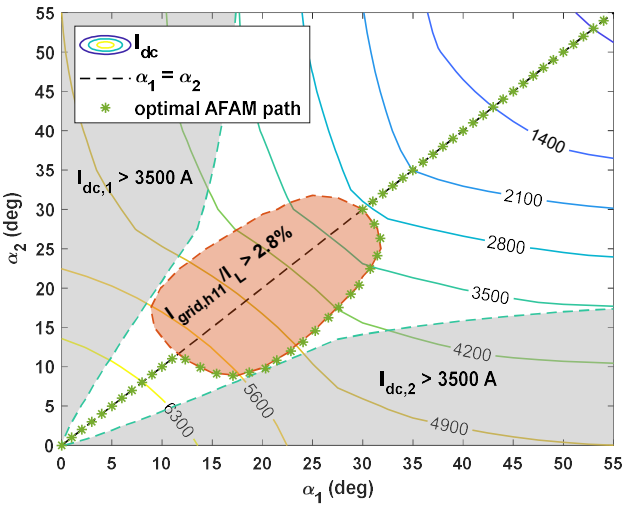

Fig. 7. Optimal AFAM $\alpha_1 - \alpha_2$ path for minimizing L_{ac} and comply with IEEE 519-2014 grid current harmonic limits.

SFAM cannot be followed as the 11th harmonic of the grid current would surpass its corresponding regulation limit. In this range, however, it is possible to use AFAM in order to comply with regulation. Furthermore, as it is shown in Fig. 7, the optimal $\alpha_1 - \alpha_2$ AFAM path is the one that follows the isoline of this regulation limit, as it is the closest path to the SFAM line, and therefore the one with lower current unbalance between the two bridges and consequently lower 5th and 7th harmonics.

Thanks to this AFAM, the required L_{ac} inductance has been reduced from 130 µH (corresponding to the typical SFAM) down to 50 µH, that is, a 62% reduction. As a result, the reactive power consumption of the thyristor rectifier (Q_t) is lowered from 3.9 MVAr to 2.7 MVAr. Using the equations developed in Appendix, the apparent power of the STATCOM (S_s) has been calculated. Fig. 8, shows the required S_s as a function of I_{dc} for the 12-pulse thyristor rectifier using SFAM and AFAM (each of them with their corresponding L_{ac} inductance value). The maximum S_s is equal to 3.9 MVA in the SFAM case and 2.7 MVA in the AFAM case, that is, a reduction of 31%. These results are also compared to the 6-pulse thyristor rectifier what was analyzed in [5], in which a maximum S_s of 3.6 MVA is required. This shows that the STATCOM power needed to achieve unity power factor and compensate 5th and 7th current harmonics is lower in the 12-pulse rectifier with AFAM than in the 6-pulse rectifier.

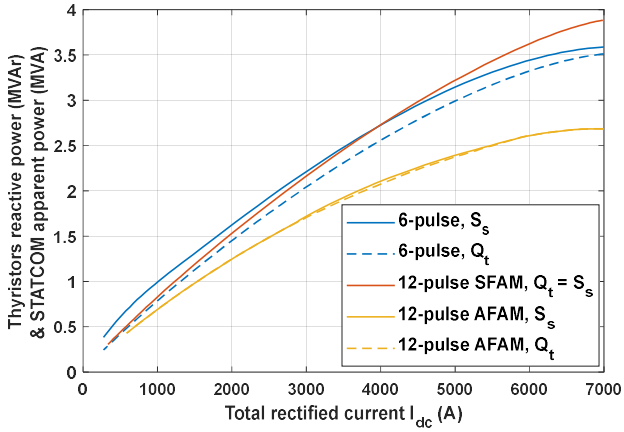

Fig. 8. Required apparent power of the STATCOM as a function of the electrolyzer current, for the 6-pulse thyristor rectifier and 12-pulse rectifier using SFAM and AFAM.

Fig. 8 also shows the reactive power consumption of the 12-pulse and 6-pulse thyristor rectifiers (Q_t). In the 12-pulse SFAM case, this Q_t is equal to S_s, as there are no 5th and 7th harmonics that need to be filtered with the STATCOM; whereas in the 6-pulse and 12-pulse AFAM cases, it is demonstrated that the required power to filter these 5th and 7th harmonics is almost negligible compared to the reactive power compensation, as S_s is only slightly higher than Q_t.

VI. Conclusion

In this paper, an AFAM strategy is proposed for 12-pulse thyristor rectifiers supplying high-power electrolyzers. It has been demonstrated that thanks to this AFAM it is possible to lower the 11th and 13th grid current harmonics, and consequently reduce the size of the filtering inductances required to meet the regulation limits for these specific harmonics, which are the most restrictive ones in 12-pulse rectifiers. In addition, 5th and 7th harmonics that arise as a result of the firing angle imbalance between the two 6-pulse bridges can be easily filtered with industrial-scale STATCOMs due to their lower frequency. Furthermore, it has been proven that the reduction in reactive power consumed by the thyristor rectifier thanks to the lower ac-side inductances is way more significant than the apparent power required to filter these 5th and 7th harmonics, which translates into a reduction in STATCOM size.

The procedure to determine the optimal AFAM strategy for a given electrolyzer with the aim of minimizing passive power filters and STATCOM size has been explained. Thanks to this, the overall cost of the power converter can be considerably reduced, which is one of the keys to minimizing the capex of electrolysis systems and, consequently, the cost of green hydrogen production.

Appendix

In order to calculate the apparent power of the STATCOM, the ac current i_s flowing through it must be first determined. As it can be seen in Fig. 1, this current is equal to the difference between the desired grid current, i_g, and the one corresponding to the thyristor rectifier, i_t. This i_t, which results from the sum of the ac-side currents of the two thyristor bridges, can be expressed as:

$$i_t = \sqrt{2}\, I_{t,1} \sin(\omega t + \varphi_1) + i_{t,h}, \tag{2}$$

where $I_{t,1}$ is the RMS value of the fundamental current, φ_1 is the phase-shift of the fundamental current with respect to the grid phase voltage (and is equal to the PF if no STATCOM is used), and $i_{t,h}$ is the sum of all the higher order harmonics:

$$i_{t,h} = \sum_{n=1}^{\infty} \sqrt{2}\ I_{t,h(6n\pm1)} \sin[(6n \pm 1)\omega t + \varphi_{6n\pm1}]. \tag{3}$$

In order to achieve unity PF at the PCC, the fundamental component of the grid current i_g must present no phase-shift with respect to the grid phase voltage. Therefore, i_g can be expressed as:

$$i_g = \sqrt{2}\, I_{g,1} \sin(\omega t) + i_{g,h}, \tag{4}$$

where $I_{g,1}$ is the RMS value of the fundamental grid current and $i_{g,h}$ is the sum of all the higher order harmonics. These are equal to the thyristor harmonics $i_{t,h}$ except for the 5th and 7th (which appear only with AFAM), as these ones are filtered with the STATCOM. Therefore:

$$i_{g,h} = \sum_{n=2}^{\infty} \sqrt{2}\ I_{t,h(6n\pm1)} \sin[(6n \pm 1)\omega t + \varphi_{6n\pm1}], \tag{5}$$

These harmonics must comply with the regulation limits, which is achieved by the proper sizing of the filtering inductance L_{ac}.

The fundamental component of the grid current depends on the power consumed by the electrolyzer (P_E) and the grid phase-to-phase voltage (U_g). For unity PF:

$$I_{g,1} = \frac{P_E}{\sqrt{3}\, U_g}. \tag{6}$$

The current flowing through the STATCOM (i_s) is equal to the difference between i_g and i_t:

$$i_s = i_g - i_t. \tag{7}$$

This current therefore presents a component at the fundamental frequency, $i_{s,1}$, and the 5th and 7th harmonics of the thyristor rectifier in the case of AFAM.

$$i_s = i_{s,1} - i_{t,h5} - i_{t,h7}. \tag{8}$$

The fundamental $i_{s,1}$ presents the following expression:

$$i_{s,1} = \sqrt{2}\, I_{g,1} \sin(\omega t) - \sqrt{2}\, I_{t,1} \sin(\omega t + \varphi_1). \tag{9}$$

It can be proven that the RMS value of $i_{s,1}$ is equal to:

$$I_{s,1} = \sqrt{I_{g,1}^2 + I_{t,1}^2 - 2 I_{g,1} I_{t,1} \cos\varphi_1}. \tag{10}$$

Then, the RMS value of the total STATCOM current, I_s, can be calculated as:

$$I_s = \sqrt{\sum_{n=1}^{\infty} I_{s,hn}^2}, \tag{11}$$

$$I_s = \sqrt{I_{g,1}^2 + I_{t,1}^2 - 2 I_{g,1} I_{t,1} \cos\varphi_1 + I_{t,h5}^2 + I_{t,h7}^2}. \tag{12}$$

Finally, the total apparent power of the STATCOM (S_s) can be determined as [17]:

$$S_s = \sqrt{3}\, U_g\, I_s. \tag{13}$$

References

[1] A. Iribarren *et al.*, "Dynamic modeling of a pressurized alkaline water electrolyzer: a multiphysics approach," *IEEE Transactions on Industry Applications*, 2023, doi: 10.1109/TIA.2023.3247405.

[2] I. Dincer, "Green methods for hydrogen production," *Int. J. Hydrogen Energy*, vol. 37, no. 2, pp. 1954-1971, 2012, doi: 10.1016/j.ijhydene.2011.03.173.

[3] O. Schmidt, A. Gambhir, I. Staffell, A. Hawkes, J. Nelson, and S. Few, "Future cost and performance of water electrolysis: An expert elicitation study," *Int. J. Hydrogen Energy*, vol. 42, no. 52, pp. 30470-30492, 2017, doi: 10.1016/j.ijhydene.2017.10.045.

[4] A. Ursúa, L. Marroyo, E. Gubía, L. M. Gandía, P. M. Diéguez, and P. Sanchis, "Influence of the power supply on the energy efficiency of an alkaline water electrolyser," *Int. J. Hydrogen Energy*, vol. 34, no. 8, pp. 3221-3233, 2009, doi: 10.1016/j-ijhydene.2009.02.017.

[5] A. Iribarren *et al.*, "Modelling and operation of 6-pulse thyristor rectifiers for supplying high power electrolyzers," *2022 IEEE 23rd Workshop on Control and Modeling for Power Electtronics (COMPEL)*, Tel Aviv, Israel, pp. 1-8, 2022, doi: 10.1109/COMPEL53829.2022.9829992.

[6] B. Yodwong, D. Guilbert, M. Phattanasak, W. Kaewmanee, M. Hinaje, and G. Vitale, "AC-DC converters for electrolyzer applications: State of the art and future challenges," *Electron.*, vol. 9, no. 6, 2020, doi: 10.3390/electronics9060912.

[7] J. Koponen, V. Ruuskanen, A. Kosonen, M. Niemela, and J. Ahola, "Effect of converter topology on the specific energy consumption of alkaline water electrolyzers," *IEEE Trans. Power Electron.*, vol. 34, no. 7, pp. 6171–6182, 2019, doi: 10.1109/TPEL.2018.2876636.

[8] J. R. Rodríguez et al., “Large current rectifiers: State of the art and future trends,” *IEEE Trans. Ind. Electron.*, vol. 52, no. 3, pp. 738–746, 2005, doi: 10.1109/TIE.2005.843949.

[9] IRENA, “Green hydrogen cost reduction,” *International Renewable Energy Agency*, 2020

[10] E. Kontos, G. Tsolaridis, R. Teodorescu, and P. Bauer, “High order voltage and current harmonic mitigation using the modular multilevel converter STATCOM,” *IEEE Access*, vol. 5, pp. 16684–16692, 2017, doi: 10.1109/ACCESS.2017.2749119.

[11] D. Bernet and M. Hiller, “Integrating voltage-source active filters into diode front-end rectifiers – Harmonic mitigation and power factor correction,” *2021 23rd Eur. Conf. Power Electron. Appl. EPE 2021 ECCE Eur.*, pp. 1-9, 2021, doi: 10.23919/epe21ecceeurope50061.2021.9570531.

[12] M. Keddar, Z. Zhang, and C. Periasamy, “Power quality improvement for 20 MW PEM water electrolysis system,” *Int. J. Hydrogen Energy*, vol. 47, no. 95, pp. 40184–40195, 2022, doi: 10.1016/j.ijhydene.2022.08.073.

[13] IEEE, “IEEE recommended practice and requirements for harmonic control in electric power systems,” in *IEEE Std 519-2014*, *IEEE Power & Energy Society*, 2014, doi: 10.1109/IEEESTD.2014.6826459.

[14] J. Solanki, N. Fröhleke, and J. Böcker, “Implementation of hybrid filter for 12-pulse thyristor rectifier supplying high-current variable-voltage DC load,” *IEEE Trans. Ind. Electron.*, vol. 62, no. 8, pp. 4691–4701, 2015, doi: 10.1109/TIE.2015.2393833.

[15] W. McMurray, “A study of asymmetrical gating for phase-controlled converters,” *IEEE Transactions on Industry Applications*, vol. IA-8, no. 3, pp.289-295, 1972, doi: 10.1109/TIA.1972.349759.

[16] A. Das, J. K. Chatterjee and A. K. Gaja, "Asymmetrical firing of 12-pulse converter for controlled P-Q operation using PIC microcontroller," *2006 IEEE Power India Conference*, New Delhi, India, 2006, pp. 5 pp.-, doi: 10.1109/POWERI.2006.1632602

[17] IEEE, “Standard definitions for the measurement of electric power quantities under sinusoidal, nonsinusoidal, balanced, or unbalanced conditions 1549-2010,” *IEEE Power & Energy Society*, 2010.